Copper Nanoparticles Stabilized By Reduced Graphene Oxide as a Probe For Flectrochemical Determination of Acyclovir

Azar Sa'adi[1], Javad Shabani Shayeh[2], Zarrin Es'haghi*[1]

1. Department of Chemistry, Payame Noor University, P.O. Box 19395-4697,Tehran, Iran

2. Protein Research Center, Shahid Beheshti University, Tehran, Iran

Abstract

The electro-oxidation of acyclovir (ACV) was studied using synthesized Cu nanoparticles stabilized by reduced graphene oxide (Cu/RGO) modified carbon paste electrodes. In this work, leaf extract of rosemary (Rosmarinus officinalis) used as a reducing and stabilizing agent for biosynthesis of copper nanoparticles. The Cu/RGO nanocomposite was authorized by X-ray diffraction (XRD), Fourier transformed infrared (FT-IR) spectroscopy, `Scanning electron microscopy (SEM), and Transmission electron microscopy (TEM). In an alkaline solution, the electrochemical performance of Cu/RGO was checked and afterward utilized to make a modified carbon paste electrode to study the electrocatalytic oxidation of acyclovir, compared to copper modifier only. Two used methods for surveying of the oxidation reaction were cyclic voltammetry and chronoamperometry. The limit of detection for modified electrode was obtained 0.63 µM. Furthermore, the rate constant of the electrocatalytic oxidation of acyclovir was $(1.80 \pm 0.03) \times 10^5$ cm^{3}mol^{-1}s^{-1} and the electron-transfer coefficient was $(4.00 \pm 0.05) \times 10^{-6}$ Cm^2 s^{-1}.

Keywords

Copper Nanoparticles; Reduced Graphene Oxide; Rosemary Extract; Electrocatalysis; Modified Carbon Paste Electrode; Acyclovir.

1. INTRODUCTION

Graphene nanosheet has become as a new nanocrystalline support due to its high surface area (2630 m^{2}g^{-1}), excellent conductivity (103-104 Sm^{-1}), high chemical and thermal stability and low making cost [1-3]. It is made from carbon atoms with Sp^2 hybridization in a honeycomb lattice [4] Meanwhile, in recent years, nano metal and metal oxides have been the basis of many kinds of research in various fields, including electrochemistry [5-10]. Small sizes of these materials cause unique properties such as large surface area, quantum effects, superparamagnetic effect, high diffusion and electrochemical conductivity. In addition, their electrocatalytic and catalytic characteristics cause electron exchange between the reduction-oxidation species and the electrode surface.

Due to the extensive surface of graphene, it can strongly immobilize guest nanoparticles such as nano metals [11]. Also, the existence of some functional groups such as epoxide, hydroxyl, and carboxyl on each graphene oxide sheet (GO) in all directions assists to immobilization of the nanoparticles [12]. According to the above-ment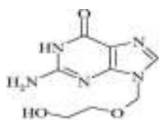ioned properties, metal ions and graphene sheets can be reduced concurrently [13-15]. Furthermore, loading of nanoparticles (NPs) on reduced graphene oxides (RGO) is prevented from their aggregation [16]. The common methods for the preparation of metal/GO or metal/RGO nanostructures are physical and chemical techniques [17-19]. These common methods aren't generally cost-effective and include utilization unsafe chemicals which are poisonous and bring ecological and biological dangers. Also, the use of chemicals such as hydrazine hydrate, sodium borohydride, and ethylene glycol to form nanometals in chemical reduction methods lead to adsorption of poisonous materials on the surface of metals and increased toxicity. Therefore, the use of more efficient, appropriate, economical and greener methods for the synthesis of metal/RGO nanocomposite is essential and inevitable.

In recent years, scientists have made great progress in the chemical synthesis of nanomaterials with specific shape and size modified with different plant extracts, fungus, and bacteria [20, 26]. In the past few years, nanomaterials have been widely used in the electro analysis of drugs [27].

Acyclovir (ACV, acycloguanosine, 9-carboxymethoxymethylguanine; Scheme 1) is the

most common antiviral medicine. It is first applied to herpes therapy, virus infections, chickenpox, and shingles.

Scheme 1. Chemical structure of acyclovir.

Some electrochemical researches have been carried out for the quantitative determination of acyclovir in medicinal and biological specimens by voltammetry methods. Different electrodes like mercury drop [28], mercury film [29], glassy carbon and ultra-trace graphite [30] and carbon paste electrodes (CPEs) were used to investigate the electrochemical behavior of acyclovir [31]. In the meantime, many advantages of CPEs such as extensive potential range, reproducibility, cost-effective, simple preparation, changeable feature and etc. have led to widespread use in electrochemical studies. By modifying CPEs with metal and RGO, the benefits of metal electrocatalytic properties and great conductivity of RGO are used simultaneously.

Regarding the above contents, in this work we used rosemary leaf extract in order to the modified synthesis of copper NPs (Cu NPs) and its stabilization by reduced graphene oxide (Cu/RGO) without the use of any surfactant and chemical stabilizer. The method is moderately environmentally friendly, non-toxic and simple. After that the electrocatalytic oxidation of acyclovir on the modified carbon paste electrode was studied by various electrochemical techniques such as cyclic voltammetry and chornoamperometry. The mentioned electrochemical sensor exhibited acceptable sensitivity towards the ACV determination with outstanding reproducibility. The sensor also is well interpreting the electrochemical behavior of ACV.

2. EXPERIMENTAL

2.1. The chemicals
All chemicals used in this work were high purity products from Merck or Aldrich Co. And were utilized without any refinement. Deionized water was used for the preparation of aqueous solutions. Acyclovir was given as a gift from Rouzdarou Co. Tehran, Iran. All experiments were done at ambient temperature.

2.2. The cell and instruments
The electrochemical trials were carried out by a potentiostat /Galvanostat (EG&G model 273) containing a common three-electrode cell with a carbon paste electrode, platinum wire, and an Ag-

AgCl as working electrode, counter electrodes, and reference electrode respectively. Surface structural identification was done by using scanning electron microscopy (SEM). X-ray diffraction (XRD) studies investigation was done by XRD-D8 (Bruker, Japan). The structure of Cu/RGO was characterized by FT-IR (Bruker, Japan). The morphology and size particle data were obtained by transmission electron microscopy (TEM- EM 10C-80 KV- ZEISS Germany).

2.3. Synthesis of Cu nanoparticles (Cu NPs)
The green synthesis of Cu NPs is summarized as: In a 500 mL flask, 30% methanol solution and 50 g of powdered rosemary leaf were added blended well. The mixture was heated to 70ºC and stirred for 30 min, then centrifuged and the supernatant solution was dissolved out of residual solid. Afterward, 15 mL of rosemary extract was added to 50 mL $CuCl_2$ solution (0.003M), after 30 min, stirring at 80ºC, the color of the reaction mixture changed, indicating the reduction of copper ions (Cu^{2+}) to Cu^0 and completion of the reaction. Then the colored suspension of Cu NPs was centrifuged for 45 min to complete settlement of Cu NPs.

2.4. Synthesis of Cu/RGO
The hard oxidation of graphite with the altered Hummers method was used for the graphite oxide synthesis [32]. Briefly, graphite powders (2.0 g) were sonicated in 98% H_2SO_4 (45 mL) for 30 min. The required amount of $KMnO_4$ (6.0 g) was slowly added to the mixture, whereas the temperature was kept below 20^0C. The mixture was then stirred at 35^0C for 2 h. After that, 90 mL of water was added to the gained solution by intensive shaking. Then 10 mL of 30% H_2O_2 solution and 130 mL of deionized water were added to the suspension. Next, an aqueous solution of HCl 5% and deionized water were consequently used to wash the gained graphite oxide suspension until the pH of the solution became neutral. Thereafter, 160 mL of water was added to the resulting graphite oxide and it was placed in an ultrasonic bath for 1h to exfoliate of the graphite oxide into the graphene oxide mono-sheets (GO).The GO powder was added to aqueous solution of $CuCl_2$ and then 15 mL extracted solution from rosemary leaves added to the system. The solution was sonicated for 1 h then this uniformly dispersed suspension was stirred for a day at 40°C. Thereafter, the final mixture was filtered and rinsed with distilled water three times. The final resultant (Cu/RGO) was dried for 12 h at 50°C.

2.5. Preparation of the working electrode
To preparation of Cu/RGO modified carbon paste electrode (denoted as Cu/RGO–CPE), the mixture

of graphite powder and Cu/RGO with a weighting ratio of (5:95) was added to deionized water, heated and stirred by a magnet to evaporate the water. Afterward, the resulting mixture and mineral oil were blended in a mortar and pestle with (75:25) ratio by hand mixing for preparation of carbon paste. The obtained paste was then compressed at the bottom of a resin tube with an area of 0.07 cm^2. A copper wire is used in the resin tube to establish the connection electrically. To produce a new electrode surface, a small ball of the paste was placed with a stainless steel rod and rubbed over a piece of weighing paper to make it appear brilliant and soft. The carbon paste electrode modified with Cu NPs (denoted as Cu-CPE) was made in a similar way.

2.6. Procedures

To prepare standard solutions of acyclovir, a certain amount of drug was dissolved in an appropriate of 1M NaOH solution (as the supporting electrolyte) and kept at 4 ^{0}C in the dark. More dilute solutions were made immediately prior to their usage. The prepared solutions were stable and their concentrations remained constant over time. The calibration curve for acyclovir in 1M NaOH solution was evaluated with the cyclic voltammetry method. The amperometric experiments were carried out in working potential of 723mV.

3. RESULT AND DISCUSSION

3.1. Characterization of the synthesized nanocomposite

The green and easy synthesized Cu NPs and Cu/RGO were identified using X-ray diffraction (XRD), FT-IR, SEM, and TEM. The crystalline structure of nanocomposite was specified by XRD. The XRD pattern of GO, Cu/RGO, and Cu NPs are shown in Fig. 1. As shown in Fig. 1a, an intense and horned peak at $2\theta = 11.2^0$ is the unique peak of GO [33] which corresponded to an interlayer spacing of about 0.76 nm, indicating the presence of oxygen functionalities, which facilitated the hydration and exfoliation of GO sheets in aqueous media. XRD pattern of Cu/RGO is shown in Fig. 1b. It is clear that, in comparison with Fig. 1a, the specific peak of GO at 11.2^0(001) disappeared. That's because after reduction, the hydrophilicity of the water-dispersed GO sheets gradually decreased, leading to an irreversible agglomeration of RGO sheets. All these results indicate that GO has been reduced to RGO during the supporting of Cu NPs on GO sheets [34]. The diffraction peaks at 42.9^0, 50.4^0 and 73.87^0 correspond to the lattice of Cu NPs respectively, attributed to Cu_2O and CuO because of the oxidation of Cu nanoparticles [35].
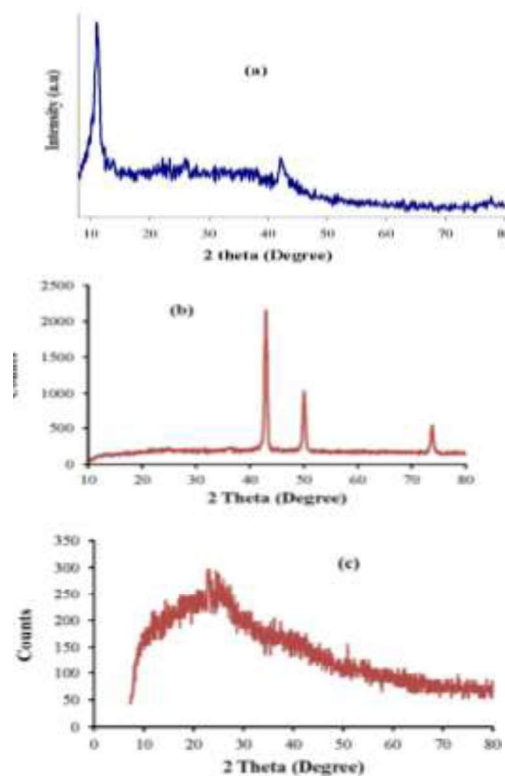

Fig. 1. XRD pattern of (a) graphene oxide, (b) Cu/ RGO and (c) Cu NPs

Fig. 1c shows that Cu NPs prepared with rosemary are amorphous that can be attributed to the agglomeration of Cu NPs. Using RGO caused to uniform distribution of Cu NPs on the surface of RGO correspond to the sharp diffraction peaks.

In order to get more direct information on particle size and morphology, TEM and SEM images were obtained. The TEM and SEM pictures of the Cu/RGO are presented in Fig. 2. It was obviously seen that the Cu NPs were distributed between RGO sheets, which indicates a good association RGO sheet with Cu NPs. Using TEM images, the diameter of the Cu NPs was around 21 nm (Fig. 2.b). SEM image of Cu NPs (Fig. 3) shows that prepared Cu NPs using rosemary extract are spherical and also some particle aggregations are clearly observed.
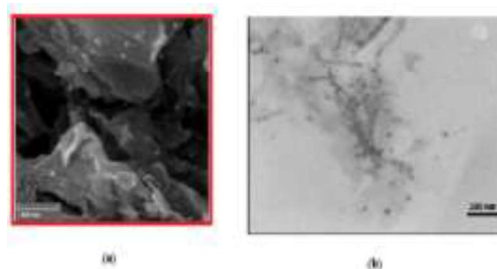

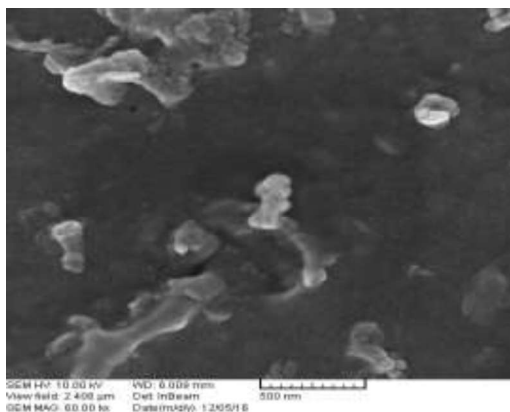**Fig. 2.** (a) SEM and (b) TEM of Cu/ RGO

Fig. 3. SEM image of Cu NPs

Fig. 4a presents the FT-IR spectra of Cu NPs to investigate the presence of functional organic groups in the surface of the Cu NPs generated by rosemary. The location of peaks at 3240, 1700, 1357, 1263 and 1075 cm^{-1} pertain to the OH functional groups, carbonyl group (C=O), stretching C=C aromatic ring, C–OH stretching vibrations and C–H stretching vibrations, respectively. Phytochemicals could be adsorbed on the surface of metal nanoparticles, possibly by interaction through π-electrons interaction in the absence of other strong ligating agents. The FT-IR spectra Cu/RGO nanocomposite are shown in Fig. 4b. The FT-IR spectrum of Cu/RGO nanocomposite highlighted that the reduction reaction eliminated the majority of oxygenated functional groups of GO, especially carboxyl groups. The present wide and strong band in the FT-IR spectrum of the Cu/RGO nanocomposite at 3536 cm^{-1} is related to the stretching vibration of O–H.
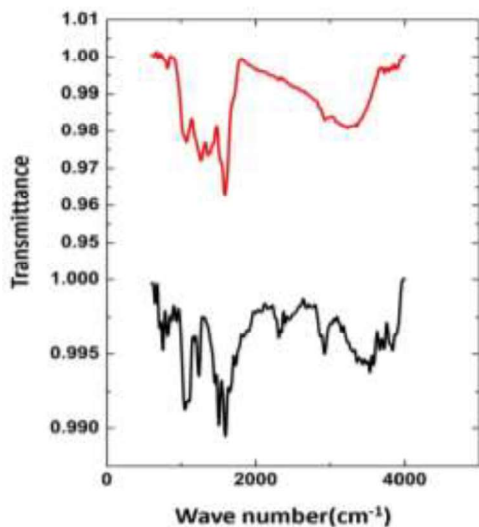

Fig. 4. FTIR of (a) Cu NPs and (b) Cu/ RGO

3.2. Cyclic voltammetric studies

Fig. 5 represents cyclic voltammograms of unmodified carbon paste electrode (un-CPE) (curve a), Cu/ CPE (curve b) and Cu/RGO-CPE (curve c) in 1M NaOH solution. The potential area was between ±1 V (Ag/AgCl) by a sweep rate of 10 mV/s. As can be seen, in the case of un- CPE no peak is observed, but voltammogram of Cu/RGO - CPE agree well with those published in the papers for copper electrodes in alkaline solutions and similar basic conditions [36-38]. In the case of copper, depending on the used potential in alkaline electrolyte, both soluble and insoluble yields including various copper oxidation species are produced [39-41]. Miller and coworkers confirmed the presence of Cu (I), Cu (II) and Cu (III) ions during anodic scanning using a ring split disk electrode and a voltammetric technique [42]. It is worth mentioning that the species produced at the electrode surface and the resulting voltammograms depend on the electrode potential, the electrolysis time, scan rate, and so on. Meanwhile, Cu (III) peak is observed at the end of anodic limit near oxygen liberation [37, 38, 43 and 44]. It can be concluded from Abdel Haleem and Ateya's proof that the Cu (III) peak is not observed at concentrations lower than 0.1 M NaOH [45]. Both Fleischmann et al. and Meyestain et al. have postulated the existence of different Cu (III) species such as the corresponding oxide (Cu$_2$O$_3$), copper oxy-hydroxide and Cu (III) radical [46, 47]. Previous studies have shown that, following an electrochemical conversion reaction Cu (II) to Cu (III) at the anodic limit of voltammograms, some of the organic compounds can be oxidized in a chemical reaction with Cu (III) species in alkaline solutions (EC' mechanism) [42,46-49]. It is also found from the comparison of curve c vs curve b (Fig.5) that currents produced by Cu/ RGO-CPE are greater than those obtained from Cu- CPE.
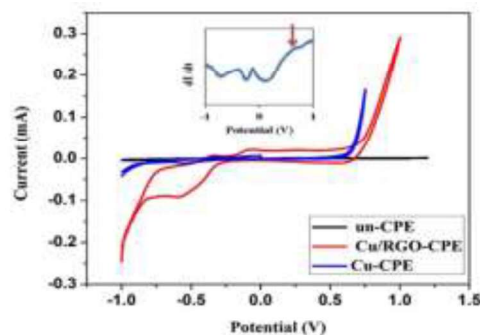

Fig. 5. Cyclic voltammograms of (a) un-CPE, (b) Cu - CPE and (c) Cu/ RGO- CPE in the potential range of -1- 1 V in 1M NaOH.The potential sweep rate was 10 mV/s Inset: Derivative voltammogram of Cu/ RGO-CPE. The arrow indicates the location of the anodic peak.

Fig. 6 shows the cyclic voltammograms of un-CPE, Cu- CPE and Cu/ RGO -CPE recorded in the presence of acyclovir (a,b,c). Acyclovir showed a very small anodic response at un-CPE while it's oxidation on both Cu/ RGO –CPE and Cu- CPE surfaces provided a single anodic peak at 723 mV and reduces cathodic peak current on the contrary scan. It was further confirmed by differential puls voltammetry technique (Fig.5, inset).
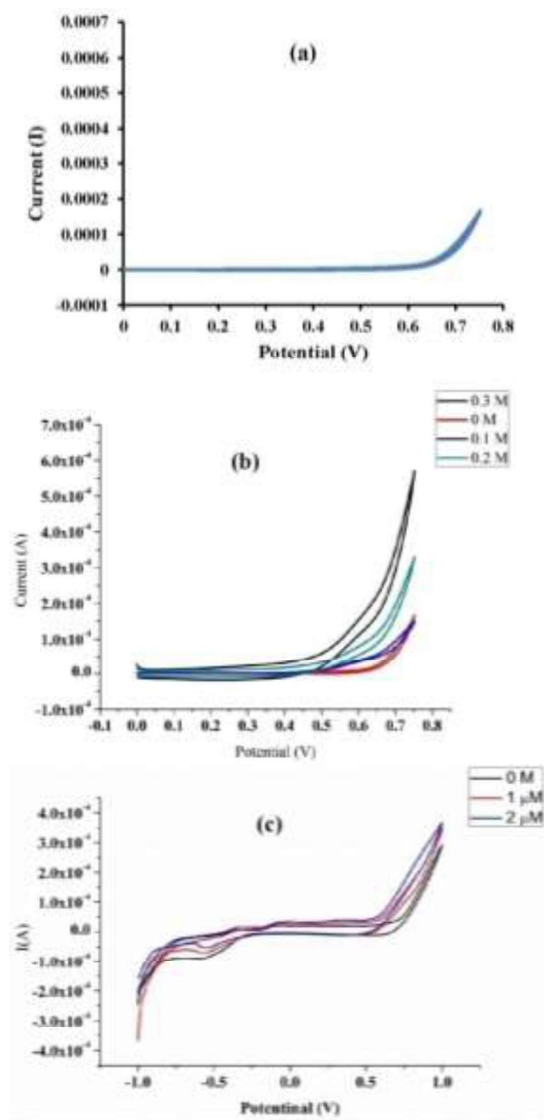

Fig. 6. Cyclic voltammograms of (a) un-CPE, (b) Cu - CPE and (c) Cu/ RGO- CPE in the presence of acyclovir in 1M NaOH.The potential sweep rate was 10 mV/s.

It should be noted that the greater anodic current density of Cu/ RGO –CPE in comparison to Cu- CPE can be attributed to the nature of the reduced graphene oxide (RGO) nanosheets with its unique properties, such as high electrical and thermal conductivity and high specific surface area. These

curves indicate that Cu/ RGO performed the electro-oxidation reaction of acyclovir more effective than those of only Cu nanoparticles both from thermodynamics and kinetics viewpoint, therefore, in subsequent experiments, we only used Cu/ RGO –CPE. The results of Fig.7 show that by increasing the concentration of acyclovir, the anodic current increases on the Cu/ RGO –CPE. This increase is observed in the near range or added to the peak potential related to Cu (II) /Cu (III) redox couple, which confirms the participation of Cu (III) species as a catalyst in the acyclovir electro-oxidation process.
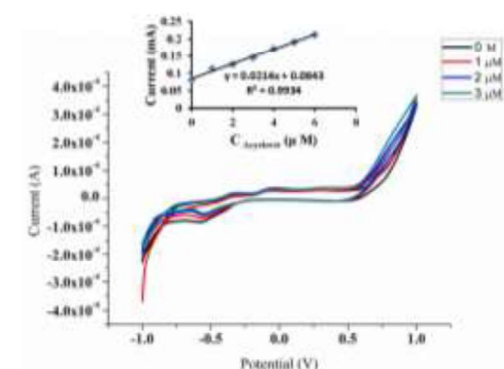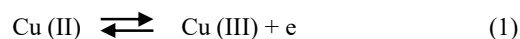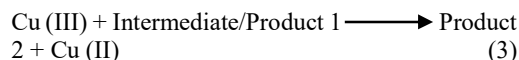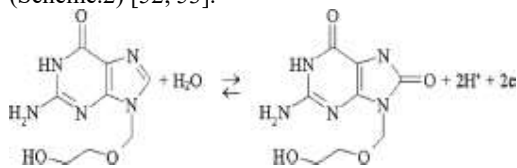

Fig. 7. Cyclic voltammograms of Cu/ RGO- CPE electrode in 1M NaOH solution with different concentrations of the acyclovir (0-3 μ M) in scan rate 10 mV/s. The inset shows the dependency of the anodic peak current on the concentration of acyclovir in solution.

Kano et al. [37] found that the presence of CuO in any two-electron oxidation reaction is essential, although it does not directly participate in the carbohydrates oxidation reaction, and some higher Cu (II) oxides (CuO$^+$ or CuOOH) act as a catalyst in the chemical reaction. In addition, there have been many reports of the role of oxidation-reduction intermediates of various copper species in the oxidation of some compounds in copper or copper-based electrodes [40-42, 43, 46-48]. For example, Helli et.al [50, 51] investigated the catalytic effect of Cu (III) species in the oxidation of acyclovir and etidronate and confirmed the hypothetical electrochemical mechanism, in which rate-limiting step included the chemical reaction of copper species with organic compounds and the formation of intermediate substances, or products. The proposed mechanism for multi-stage acyclovir oxidation on Cu/ RGO –CPE based on the above results is as follows:

$$\text{Cu (II)} \rightleftharpoons \text{Cu (III)} + \text{e} \qquad (1)$$

Cu (III) + Acyclovir $\longrightarrow$ Intermediate/Product 1+ Cu (II) (2)

K_{cat2}

Cu (III) + Intermediate/Product 1 ⟶ Product 2 + Cu (II)   (3)
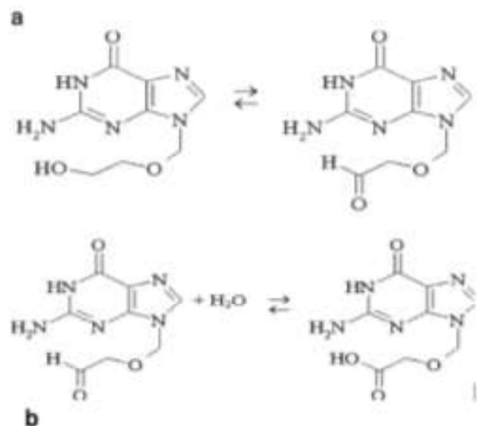
It turns out that the anodic signal generated in the electrode, resulting from the simultaneous or multi-stage oxidation of one or more functional groups in the acyclovir structure. Since acyclovir is synthesized from nucleic acid guanine, it can be oxidized to the corresponding oxoguanine (Scheme.2) [52, 53].

Scheme 2. Oxidation of acyclovir to the corresponding oxo-guanine analog.

Another hypothesis is that for the transfer of electrons from acyclovir to Cu (III), the formation of a metal alkoxide between the alcoholic oxygen and soluble Cu (III) ions to produce radical intermediate and Cu (II) is inevitable. The radicals should be oxidized immediately and, according to the reactions shown in Scheme.3, alcohol of type one is converted to an aldehyde or corresponding carboxylic acid [54].

Scheme 3. Oxidation of acyclovir to the corresponding aldehyde (a) and/or carboxylic acid (b).

Meanwhile, Cu (II) ions are oxidized to produce Cu (III) catalytic species. In another test, in order to confirm the high stability and resistance of Cu/ RGO –CPE, repeated cyclic voltammograms, in 0.1M NaOH containing 3 μM acyclovir was obtained by the above electrode, which showed a slight change in peak current. The results also show the electrode's resistance to the conventional problems of oxidation-based sensors [40] such as electrode fouling or accumulation of intermediate products and compounds or contamination on the electrode surface.

The plot of peak current vs. concentration is shown in Fig. 7, where the linear dependency of current peak and acyclovir concentration extends up to the concentration of 6 μM acyclovir.

The limit of detection (LOD) and quantitation (LOQ) of the procedure was calculated according to the 3 SD/m and 10 SD/m criteria, respectively, where SD is the standard deviation of the intercept and m is the slope of the calibration curve [55]. The determined parameters for the calibration curve of the drug, accuracy and precision, LOD and LOQ, and the slope of calibration curve are reported in Table 1.

Table 1. Comparison of statistical parameters of electro-catalytic oxidation of acyclovir on Cu/ RGO-CPE (n=5)

Statistical Parameters	This work	Ref. [50]	Ref.[31]
Linear range (μM)	1.0-6.0	27-521	1.4-15.7
Slope (μA.μM $^{-1}$)	21.4 ± 1.2	24.6	0.44
Intercept (A)	$(8.0\pm0.5)10^{-5}$	$(18.2)10^{-5}$	$(10.8)10^{-5}$
LOD (μM)	0.63	2.64	40
LOQ (μM)	1.0	8.8	120
RSD (%)	2.1	4.2	4.4

3.2. Chronoamperometric studies

Double potential step chronoamperometry was used to verify of the processes that took place on the basis of the EC' mechanism [48]. Double-step chronoamperograms for Cu/RGO–CPE are shown in Fig. 8. The working electrode potential is set at 723 mV (first step) and 300mV (second step) both in the lack (curve 1) and in the existence of acyclovir (curve 2-8) over a wide concentration range. The forward and reverse potential step chronoamperometry of the modified electrode in the blank solution showed an almost symmetrical chronoamperograms with almost equal charges consumed for the oxidation and reduction of surface-confined Cu (II)/ Cu (III) sites. The transient currents rise upon increasing acyclovir concentration and when the potential step took the reverse values (300 mV), no considerable currents are reached indicating that the electrocatalytic oxidation of acyclovir is irreversible. Furthermore, the transient currents declined by the time in a Cornelian manner. This indicates that the electrocatalytic oxidation of acyclovir on Cu/RGO -CPE was controlled by diffusion in the bulk of the solution.

Therefore, chronoamperometry used for evaluation of the rate of the chemical reaction between the acyclovir and modified layer (k) according to the following equation [56]:

$$I_C/I_L = \gamma^{1/2} [\pi^{1/2} \mathrm{erf}\,(\gamma^{1/2}) + \exp\,(-\gamma) / \gamma^{1/2}] \qquad (4)$$

Where I_C and I_L are the currents in the existence and lack of acyclovir, and $\gamma = kCt$ is the argument of the error function, k is the catalytic rate constant, C is the bulk concentration of acyclovir and t is the passed time. In the cases where $\gamma > 1.5$, erf $(\gamma 1/2)$ is nearly equal to one and the upper equation can be summarized to [57]:

$$I_C/I_L = \gamma^{1/2} \pi^{1/2} = \pi^{1/2} (kCt)^{1/2} \qquad [5]$$

From the slope of the I_C/I_L versus $t_{1/2}$ plot, presented in Fig. 9, inset B, the mean value of k for the concentration range of 0.4 to 3 μM of acyclovir was obtained as $(1.80 \pm 0.03) \times 10^5$ cm^{3}mol^{-1}s^{-1}.

Also, by using the slope of the line represented in Fig. 8, inset A, the diffusion coefficient of acyclovir can be obtained according to Cottrell equation [56]:

$$I = nFAD^{1/2}\pi^{-1/2} C^{1/2} t^{-1/2} \qquad (6)$$

Where D is the diffusion coefficient, the electrode surface area, C the bulk concentration and t is the elapsed time. The mean value of the diffusion coefficient for acyclovir was found to be $(4.00 \pm 0.05) \times 10^{-6}$ cm^2 s^{-1}.
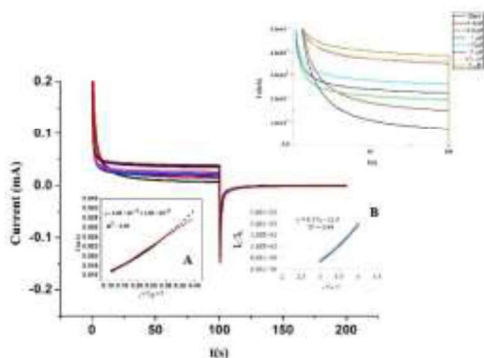

Fig. 8. Double steps choronoamperograms of Cu/ RGO-CPE electrode in 1M NaOH solution with different concentrations of the acyclovir of: (a) 0 M, (b) 0.4 μ M, (c) 0.8 μ M, (d) 1 μ M, (e) 1.5 μ M, (f) 2 μ M, (g) 2.5 μM and (h) 3 μM acyclovir. Potential steps were 723 mV and 300 mV, respectively. *Inset A* dependence of transient current (e) on $t^{-1/2}$. *Inset B* depence of I_C/I_L on $t^{1/2}$.

4. CONCLUSION

We have successfully synthesized Cu NPs and Cu/ RGO nanocomposite via the reduction of aqueous Cu^{2+} of Cu (0) by using rosemary leaf extract. The use of rosemary leaf extract is economic, easy access and friendly environment. Flavonoids in rosemary leaves work as a reducing and fixing agent. XRD, FT-IR, SEM, and TEM were used for characterizing of the morphology and structure of the Cu NPs and Cu/RGO nanocomposite. Also, the synthesized Cu NPs and Cu/ RGO nanocomposite were successfully used for modification of a carbon paste electrode. The altered electrode showed high catalytic activity toward the electro-oxidation of the acyclovir with a cyclic mediation electron-transfer process. The electrocatalytic activity of the Cu/ RGO- CPE was greater than that of the Cu − CPE. This is mainly due to the really large surface area and higher electrical and ionic conductivity of Cu/ RGO. An amperometric procedure was successfully progressed for the determination of the catalytic rate constant and diffusion coefficient of the acyclovir. Furthermore, the synthesized Cu NPs and Cu/ RGO nanocomposite by this way are completely durable and can be guarded below an inert atmosphere for too many months.

REFERENCES
[1] A.K. Geim and K.S. Novoselov, The rise of graphene, *Nat. Mater.* 6 (2007) 183-191.

[2] J.S. Bunch, A.M. Van Der Zande, S.S. Verbridge, I.W. Frank, D.M. Tanenbaum, J.M. Parpia, H.G. Craighead and P.L. McEuen, Electromechanical Resonators from Graphene Sheets, *Science* 315 (2007) 490-493.

[3] S. Park and R.S. Ruoff, Chemical methods for the production of graphenes, *Nat. Nanotechnol.* 4 (2009) 217-224.

[4] B.F.Machado and P. Serp, Graphene-based materials for catalysis, *Catal. Sci. Technol.* 2 (2012) 54-75.

[5] P. Zijlstra and M. Orrit, Single metal nanoparticles: optical detection, spectroscopy and applications, *Rep. Prog. Phys.* 74 (2011) 106401.

[6] B.M. Munoz-Flores, B. I. Kharisov, V. M. Jimenez-Perez, P.E. Martinez and S.T. Lopez Recent Advances in the Synthesis and Main Applications of Metallic Nanoalloys, *Ind. Eng. Chem. Res.* 50 (2011) 7705-77021.

[7] S.J. Guo and E.K. Wang, Noble metal nanomaterials: Controllable synthesis and application in fuel cells and analytical sensors, *Nano Today* 6 (2011) 240-264.

[8] G. Thirumurugan and M.D. Dhanaraju, Novel Biogenic Metal Nanoparticles for Pharmaceutical Applications, *Adv. Sci. Lett.* 4 (2011) 339-348.

[9] E. Comini and G. Sberveglieri, Metal oxide nanowires as chemical sensors, *Mater. Today*, 13 (2010) 28.

[10] A. Kolmakov and M. Moskovits, Chemical sensing and catalysis by one Dimensional metal-oxide nanostructures, *Annu. Rev. Mater. Res.* 34 (2004) 151-180.

[11] R. Muszynski, R.B. Seger and P.V. Kamat, Decorating Graphene Sheets with Gold Nanoparticles, *J. Phys. Chem. C* 112 (2008) 5263-5266.

[12] P.V. Kamat, Graphene-Based Nanoarchitectures. Anchoring Semiconductor and Metal Nanoparticles on a Two-Dimensional Carbon Support, *J. Phys. Chem. Lett.* 1 (2010) 520-527.

[13] B. Seger and P.V. Kamat, Electrocatalytically Active Graphene-Platinum Nanocomposites. Role of 2-D Carbon Support in PEM Fuel Cells, *J. Phys. Chem. C* 113 (2009) 7990.

[14] Y. Zhu, M.D. Stoller, W. Cai, A. Velamakanni, R.D. Piner and D. Chen, Exfoliation of graphite oxide in propylene carbonate and thermal reduction of the resulting graphene oxide platelets, *ACS Nano* 4 (2010) 1227-1233.

[15] I.V. Lightcap, T.H. Kosel and P.V. Kamat, Anchoring semiconductor and metal nanoparticles on a two-dimensional catalyst mat. Storing and shuttling electrons with reduced graphene oxide, *Nano Lett.* 10(2010) 577-583.

[16] Si. Yongchao and T.S. Edward, Exfoliated Graphene Separated by Platinum Nanoparticles, *Chem. Mater.* 20 (2008) 6792-6797.

[17] M. Nasrollahzadeh, F. Babaei, P. Fakhri and B. Jaleh, Synthesis, characterization, structural, optical properties and catalytic activity of reduced graphene oxide/copper nanocomposites, *RSC Adv.* 5 (2015)10782-10789.

[18] M. Bagherzadeh and A. Farahbakhsh, in: A. Tiwari, M. Syvajarvi (Eds.), *Surface functionalization of graphene, in Graphene Materials: Fundamentals and Emerging Applications*, Wiley, New York (2015).

[19] J. ShabaniShayeh, A. Ehsani, M.R. Ganjalia, P. Norouzian and B. Jalehda, Conductive polymer/reduced graphene oxide/Au nanoparticles as efficient composite materials in electrochemical supercapacitors, *Appl. Surf. Sci*. 353 (2015) 594-599.

[20] Y. Konishi, K. Ohno, N. Saitoh, T. Nomura, S. Nagamine, H. Hishida, Y. Takahashi and T. Uruga, Bioreductive deposition of platinum nanoparticles on the bacterium shewanella algae, *J. Biotechnol.* 128 (2007) 648-653.

[21] M. Rai, A. Yadav and A. Cade, Current [corrected] trends in phytosynthesis of metal nanoparticles, *Crit. Rev. Biotechnol*. 28 (2008) 277-284.

[22] E.S. Abdel-Halim, M.H. El-Rafie and S.S. Al-Deyab, Polyacrylamide/guar gum graft copolymer for preparation of silver nanoparticles, *Carbohydr. Polym.* 85 (2011) 692-697.

[23] A.R. Jasbi, Chemistry and biological activity of secondary metabolites in Euphorbia from Iran, *Phytochem.* 67 (2006) 1977-1984.

[24] S.P. Dubey, M. Lahtinen and M. Sillanpa, Tansy fruit mediated greener synthesis of silver and gold nanoparticles Process, *Biochem.* 45 (2010) 1065-1071.

[25] G. Zhan, J. Huang, M. Du, I. Abdul-Rauf, Y. Ma and Q. Li, Green synthesis of Au–Pd bimetallic nanoparticles: Single-step bioreduction method with plant extract, *Mat. Lett.* 65 (2011) 2989-2991.

[26] X. Huang, H. Wu, S. Pu, W. Zhang, X. Liao and B. Shi, One-step room-temperature synthesis of Au@Pd core-shell nanoparticles with the tunable structure using plant tannin as reductant and stabilizer, *Green Chem.* 13 (2011) 950-957.

[27] A. Rohi, K. Karimian and H. Heli, Nanostructured materials in electroanalysis of pharmaceuticals, *Anal. Biochem.* 497 (2016) 39-47.

[28] S. Skrzypek, W. Ciesielski and S. Yilmaz, Voltammetric study of aciclovir using controlled grow mercury drop electrode, *Chem. Anal.* 52 (2007) 1071-1079.

[29] A.A. Castro, A.I.P. Cordoves and P.A.M. Farias, Determination of the antiretroviral drug acyclovir in diluted alkaline electrolyte by adsorptive stripping voltammetry at the mercury film electrode, *Anal. Chem. Insights* 8 (2013) 21-28.

[30] M. Sadikoglu, G. Saglikoglu, S. Yagmur, E. Orta and S. Yilmaz, Voltammetric determination of acyclovir in human urine using ultra trace graphite and glassy carbon electrodes, *Curr. Anal. Chem.* 7 (2011) 130-135.

[31] H. Heli, F. Pourbahman and N. Sattarahmady, Nanoporous Nickel Microspheres: Synthesis and Application for the Electrocatalytic Oxidation and Determination of Acyclovir, *Anal. Sci.* 28 (2012) 503-510.

[32] A. Tajiki and M. Abdouss, Synthesis and characterization of graphene oxide nano-sheets for effective removal of copper phthalocyanine from aqueous media, *Iran. J. Chem. Chem. Eng. (IJCCE)*, 36 (2017) 1-9.

[33] Z. Xu, Y. Zhang, X. Qian, J. Shi, L. Chen, B. Li, J. Niu and L. Liu, One-step synthesis of polyacrylamide functionalized graphene and its application in Pb(II) removal, *Appl. Surf. Sci.* 316 (2014) 308–314.

[34] Z. Xiong, L.L. Zhang, J. Ma and X.S. Zhao, Photocatalytic degradation of dyes over graphene- gold nanocomposites under visible light irradiation *Chem. Commun.* 46 (2010) 6099-6101.

[35] Omar H. Abd-Elkader and N.M. Derza, Synthesis and characterization of new copper-based nanocomposite, *Int. J. Electrochem.Sci.* 8 (2013) 8614-8622.

[36] Marioli, J.M. Kuwana and T. Electrochemical characterization of carbohydrate oxidation at copper electrodes, Electrochim. Acta, 37 (1992) 1187-1197.

[37] K. Kano, M. Torimura, Y.Esaka, M. Goto and T. Ueda, Electrocatalytic oxidation of carbohydrates at copper (II)-modified electrodes and its application to flow-through detection, *J. Electroanal. Chem.* 372 (1994) 137-143.

[38] C.H. Pyun and S.M. Park, *In Situ* Spectro-electrochemical Studies on Anodic Oxidation of Copper in Alkaline Solution, *J. Electrochem. Soc.* 133 (1986) 2024-2030.

[39] J.M.M. Droog, C.A. Alderliesten, P.T. Alserliesten and G.A. Gootsma, Initial stages of anodic oxidation of poly-crystalline copper electrodes in alkaline solution, *J. Electroanal. Chem.* 111 (1980) 61-70.

[40] F. Wang, X.X. Chen and S.H. Hu, Studies on electrochemical behavior of acyclovir and its voltammetric determination with nano-structured film electrode, *Anal. Chim. Acta* 576 (2006) 17-22.

[41] M. Hajjizadeh, A. Jabbari, H. Heli and A.A. Moosavi-Movahedi, Electrooxidation and determination of mefenamic acid and indomethacin using a copper electrode, *Chem. Anal.* 53 (2008) 429- 444.

[42] B. Miller, Split-Ring Disk Study of the Anodic Processes at a Copper Electrode in Alkaline Solution, *J. Electrochem. Soc.* 116 (1969) 16750-17680.

[43] L.D. Burke, M.J.G. Ahern and T.G. Ryan, An Investigation of the Anodic Behavior of Copper and Its Anodically Produced Oxides in Aqueous Solutions of High pH, *J. Electrochem. Soc.* 137 (1990) 553-561.

[44] I.G. Casella and M. Gatta, Anodic electrodeposition of copper oxide/hydroxide films by alkaline solutions containing cuprous cyanide ions, *J. Electroanal. Chem.* 494 (2000) 12-20.

[45] S.M. Abd el Haleem and B.G. Ateya, Cyclic voltammetry of copper in sodium hydroxide solutions, *J. Electroanal. Chern.* 117 (1981) 309-319.

[46] M. Fleischmann, K. Korinek and D. Pletcher, The kinetics and mechanism of the oxidation of amines and alcohols at oxide-covered nickel, silver, copper, and cobalt electrodes, *J. Chem. Soc.* 2 (1972) 1396-1403.

[47] D. Meyerstein, F.M. Hawkridge and T. Kuwana, The spectro-electrochemical characterization of the electrocatalytic oxidation of Cu (II) ethylenediamine, *J. Electroanal. Chem.* 40 (1972) 377-384.

[48] H. Heli, M. Hajjizadeh, A. Jabbari and A.A. Moosavi-Movahedi, Copper nanoparticles-modified carbon paste transducer as a biosensor for determination of acetylcholine, *Biosens. Bioelectron.* 24 (2009) 2328-2333.

[49] H. Heli, M. Hajjizadeh, A. Jabbari and A.A. Moosavi-Movahedi, Fine steps of electrocatalytic oxidation and sensitive detection of some amino acids on copper nanoparticles, *Anal Biochem.* 388 (2009) 81-90.

[50] H. Heli, M. Zarghan, A. Jabbari, A. Parsaei and A.A. Moosavi-Movahedi, Electrocatalytic oxidation of the antiviral drug acyclovir on a copper nanoparticles-modified carbon paste electrode, J. Solid State Electrochem. 14 (2010) 787-795.

[51] H. Heli, F. Faramarzi, A. Jabbari, A.Parsaei and A.A. Moosavi-Movahedi, Electrooxidation and determination of etidronate using copper nanoparticles and microparticles-modified carbon paste electrodes, *J. Braz. Chem. Soc.* 21 (2010) 16-24.

[52] K.C. Honeychurch, M.R. O'Donovan and J.P. Hart, Voltammetricbehaviour of DNA bases at a screen-printed carbon electrode and its application to a simple and rapid voltammetric method for the determination of oxidative damage in double-stranded DNA, *Biosens. Bioelectron.* 22 (2007) 2057-2064.

[53] E. Gonzalez-Fernandez, N. de-Los Santos-Alvarez, M.J. Lobo-Castanon, A.J. Miranda-Ordieres and P. Tunon-Blanco, Electrochemical Oxidation of Guanosine and Xanthosine at Physiological pH: Further Evidences of a Convergent Mechanism for the Oxidation of Purine Nucleosides, *Electroanalysis* 20 (2008) 833-839.

[54] O. Hammerich, J.H.P. Utley and L. Eberson, *Organic electrochemistry*, Marcel Dekker, New York (1991).

[55] J.C. Miller and J.N. Miller, Statistics for analytical chemistry, Fourth ed., Ellis-Harwood, New York (1994) pp. 115.

[56] A.J. Bard and L.R. Faulkner, *Electrochemical methods*, Wiley, New York (2001).

[57] J. Raoof, A. Omrani, R. Ojani, F. Monfared, Poly (N-methyl aniline)/ nickel modified carbon paste electrode as an efficient and cheap electrode for electrocatalytic oxidation of formaldehyde in alkaline medium, *J. Electroanal. Chem.* 633 (2009) 153-158.

نانو ذرات مس تثبیت‌شده بر روی اکسید گرافن احیاشده به عنوان یک ردیاب برای اندازه گیری الکتروشیمیایی آسیکلوویر

آذر سعدی[۱]، جواد شعبانی شایه[۲]، زرین اسحاقی[۱و]*

۱. گروه شیمی، دانشگاه پیام نور، تهران، ایران

۲. مرکز تحقیقات پروتئین دانشگاه شهید بهشتی، تهران، ایران

چکیده

الکترواکسیداسیون آسیکلوویر با استفاده از الکترودخمیری کربن اصلاح‌شده با نانو ذرات مس سنتزی تثبیت‌شده بر روی اکسیدگرافن احیاشده (Cu/RGO) مطالعه شد. در این مطالعه، از عصاره برگ رزماری به عنوان عامل کاهنده و تثبیت‌کننده برای بیوسنتز نانوذرات مس استفاده شد. برای شناسایی ساختار نانوذرات و نانو کامپوزیت سنتز شده از XRD، FT-IR، SEM و TEM استفاده شد. عملکرد الکتروشیمیایی Cu/RGO در محلول قلیایی بررسی شد و پس از آن برای اصلاح الکترود خمیری کربن برای مطالعه اکسیداسیون الکتروکاتالیتیکی آسیکلوویر استفاده گردید و با اصلاح‌گر مس به تنهایی مقایسه شد. از روش‌های ولتامتری چرخه‌ای و کرونوآمپرومتری برای مطالعه مکانیسم اکسیداسیون و تعیین ثابت سرعت الکتروکاتالیتیکی و ضریب نفوذ آسیکلوویر استفاده شد. حد تشخیص الکترود اصلاح‌شده ۰/۶۳ میکرومولار بود. علاوه برآن، ثابت سرعت اکسیداسیون الکتروکاتالیتیکی آسیکلوویر (1.8 ± 0.03)×$10^5 cm^3\ mol^{-1} s^{-1}$ و ضریب انتقال الکترون، (4 ± 0.05)×$10^{-6} cm^2 s^{-1}$ محاسبه شد.

واژه‌های کلیدی

نانو ذره مس؛ اکسید گرافن احیاشده؛ عصاره رزماری؛ الکتروکاتالیز؛ الکترود خمیری کربن اصلاح‌شده؛ آسیکلوویر.